Journal of Computational Acoustics, Vol. 9, No. 3 (2001) 1015–1023

SCALE AND ANGLE DEPENDENT REFLECTION PROPERTIES OF SELF-SIMILAR INTERFACES*

JEROEN GOUDSWAARD and KEES WAPENAAR
Delft University of Technology, Centre for Technical Geoscience, P.O. Box 5028, 2600 GA Delft, The Netherlands

Received 30 June 1999
Revised 6 March 2000

We propose an alternative parameterization of seismic reflectors in the subsurface, in terms of self-similar singularities, which are generalizations of stepfunctions. This parameterization captures the multi-scale behavior of real sonic P-wave velocity logs, as can be derived by performing modulus maxima analysis on wavelet-transformed well-logs. Results on synthetic seismic reflection data, modeled in real well-logs, show that a singularity parameter can be retrieved, that is consistent with the parameter derived directly from the well-log.

1. Introduction

Strong reflections in seismic data can often be matched with sharp outliers in the velocity function of the earth's subsurface. This velocity function is generally known by means of the sonic P-velocity log, measured in the borehole (hereafter referred to as well-log). The usual description of layering in the earth is by means of stepfunctions, by which only an approximated version of the outliers can be constructed. Mallat and Hwang[1] have discovered that the zooming property of the continuous wavelet transform can be used to perform regularity analysis and singularity detection on all kinds of measurements. Herrmann[2] has shown that well-logs can be analyzed for the presence of singularities by means of this transform, thus showing that well-logs exhibit singular behavior over a broad scale range. This implies that a well-log cannot be parameterized effectively by stepfunctions alone. In this paper we discuss an alternative parameterization of seismic reflectors, in terms of self-similar singularities, which are a generalization of stepfunctions. Reflectors described by this parameterization are singular in the same spectral range as real well-logs. Furthermore we will show how to extract a singularity parameter which quantifies this singular behavior in a consistent way from both the well-log as well as from seismic reflection data. It is noteworthy to mention that in Dessing[3] similar parameterizations for reflectors have been analyzed together with the instantaneous phases of the reflection responses on these reflectors.

*Presented at ICTCA'99, the 4th International Conference on Theoretical and Computational Acoustics, May 1999, Trieste, Italy.

2. Extraction of Singularity Parameters from the Well-Log

In this section, we review the procedure proposed by Herrmann[2] for analyzing the scaling properties of the wavelet transform of reflectors in well-logs and we show how to obtain a singularity parameter α from the wavelet transformed well-log. The analysis is very much along the lines proposed by Mallat and Hwang.[1] Figure 1(a) shows a P-wave velocity log sampled with 15 cm (0.5 ft) spacing. Note the rapid variations in the velocity field and many sharp outliers. As an analysis tool we use the continuous wavelet transform

$$\check{c}(\sigma, z) = \frac{1}{|\sigma|^{\mu}} \int_{-\infty}^{\infty} c(z')\psi\left(\frac{z'-z}{\sigma}\right) \mathrm{d}z' \,, \tag{2.1}$$

which is a convolution of the velocity function $c(z)$ with scalable wavelets $\psi(z/\sigma)$. In this representation the scale σ introduces a contraction or a stretching of the wavelet, which makes it possible to zoom in (or out) on irregular features of the well-log (μ is a normalization coefficient that has been set to 1 in this example). The wavelet transform can be seen as a localized frequency decomposition of the function $c(z)$. Figures 1(b) and 1(c) are both representations of the continuous wavelet transform. In Fig. 1(c) the neighboring maxima

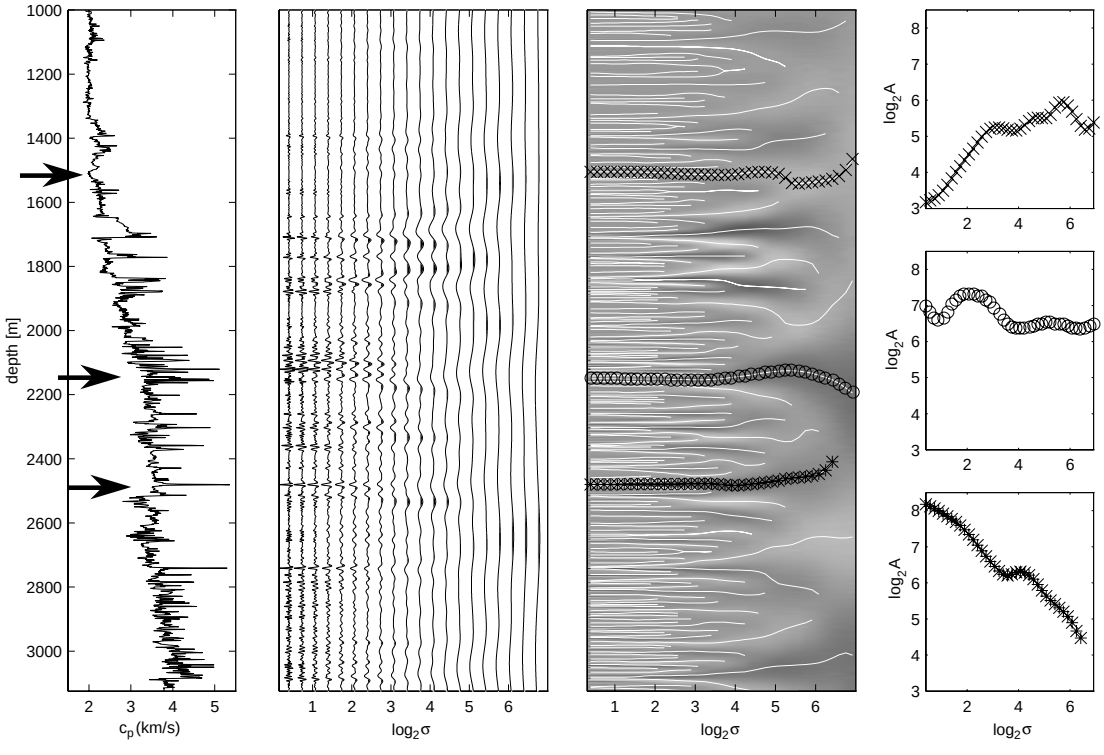

Fig. 1. Multi-scale analysis of a well-log.[2] (a) The original well-log (courtesy Mobil); (b) The Continuous Wavelet Transform of the well-log in (a); (c) Modulus maxima lines, obtained from the modulus of (b); (d) Double-logarithmic plots of the amplitudes A along the depicted modulus maxima lines in (c). A positive, a zero and a negative slope (singularity strength) can be discerned.

are connected by so-called modulus maxima lines. Figure 1(d) shows the amplitude behavior of the wavelet transform along the depicted modulus maxima lines.

We can see that not only a scale independent reflector is visible (slope=0) but also reflectors which have a slope which is negative or positive. This means that these reflectors are scale dependent and cannot be described by stepfunction interfaces. As the slope along the modulus maxima lines is reasonably constant, we will parameterize the main reflectors in a well-log by shifted versions of self-similar functions of the form

$$c(z) = \begin{cases} c_1 |z/z_1|^\alpha & \text{for } z < 0 \\ c_2 |z/z_2|^\alpha & \text{for } z > 0\,, \end{cases} \tag{2.2}$$

for which we will show that the wavelet transform exhibits a similar constant slope behavior. Note that for the special case of $\alpha = 0$, Eq. (2.2) defines a stepfunction from c_1 to c_2.

For arbitrary α, the scaling behavior of this self-similar singularity reads

$$c(\sigma z) = \sigma^\alpha c(z)\,, \tag{2.3}$$

for $\sigma > 0$. The wavelet transform $\check{c}(\sigma, z)$ of this singularity is defined by Eq. (2.1). Replacing z by σz, z' by $\sigma z'$ and using Eq. (2.3) for $\sigma > 0$ we arrive at

$$\check{c}(\sigma, \sigma z) = \sigma^{\alpha+1-\mu} \int_{-\infty}^{\infty} c(z')\psi(z' - z)\mathrm{d}z'\,, \tag{2.4}$$

or, comparing the right-hand side with that of Eq. (2.1) for $\sigma = 1$,

$$\check{c}(\sigma, \sigma z) = \sigma^{\alpha+1-\mu} \check{c}(1, z)\,. \tag{2.5}$$

Let $z = z_{\max}$ denote the z-value for which $|\check{c}(1, z)|$ reaches a local maximum. Substitution in Eq. (2.5) gives

$$\check{c}(\sigma, \sigma z_{\max}) = \sigma^{\alpha+1-\mu} \check{c}(1, z_{\max})\,. \tag{2.6}$$

Taking the logarithm of the modulus of both sides of Eq. (2.6) yields the following expression for the logarithm of the amplitudes along a modulus maxima line:

$$\log_2 |\check{c}(\sigma, \sigma z_{\max})| = (\alpha + 1 - \mu) \log_2 \sigma + \log_2 |\check{c}(1, z_{\max})|\,. \tag{2.7}$$

For $\mu = 1$ we obtain

$$\log_2 |\check{c}(\sigma, \sigma z_{\max})| = C + \alpha \log_2 \sigma\,, \tag{2.8}$$

with $C = \log_2 |\check{c}(1, z_{\max})|$. According to Eq. (2.8), the slope of the amplitudes along the modulus maxima lines is defined by α, where α is the singularity exponent of the self-similar function defined in Eq. (2.2). Note that a constant amplitude along a modulus maximum line (i.e., $\alpha = 0$) corresponds to a stepfunction, hence, any nonzero slope identifies a singularity other than the stepfunction. It is interesting to see that the analyzed singularities in the real well-log of Fig. 1 reveal an amplitude-versus-scale behavior approximately described by Eq. (2.8).

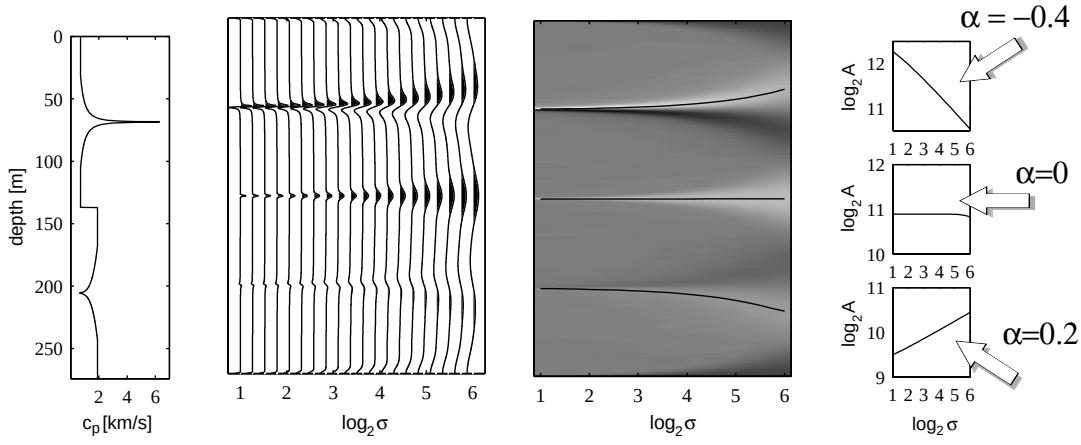

(a) (b) (c) (d)

Fig. 2. (a) Synthetic well-log; (b) wavelet transform of well-log; (c) position of modulus maxima lines in wavelet transform; (d) log–log plot of amplitude A along modulus-maxima lines versus scale: (top) $\alpha = -0.4$, (middle) $\alpha = 0$, (bottom) $\alpha = 0.2$.

Now we will test the parameterization by constructing a synthetic velocity function as in Fig. 2(a), which consists of two shifted versions of the singularity as in Eq. (2.2), which are characterized by a scaling exponent α of -0.4 and 0.2 respectively, and $c_1 = c_2$ for both singularities. The stepfunction in between the two singularities can also be seen as a singularity, but its scaling exponent α must then be chosen equal to 0, but in this case $c_1 \neq c_2$. The analyzing wavelet ψ has been chosen to be the first derivative of the Gaussian window.

Figures 2(b) and 2(c) show the same analysis as in Figs. 1(b) and 1(c). For the chosen wavelet ψ, the scale range of the analysis ($\sigma \in [4, 64]$, or to be consistent with the σ-axes in Figs. 1(b)–1(d) and 2(b)–2(d), $\log_2 \sigma \in [2, 6]$) is approximately equivalent to the bandwidth of a seismic wavelet in surface seismics. Figure 2(d) shows the amplitude-slope along the corresponding modulus maxima lines of Fig. 2(c). It shows that the singularity exponent α from Eq. (2.2) can be retrieved as the value of this slope, in accordance with Eq. (2.8).

3. Extraction of Singularity Parameters from Angle-Dependent Seismic Data

The foregoing section showed a method for retrieving a singularity parameter α from a well-log. In this section, we will introduce a method for the extraction of the same singularity parameter α from seismic reflection data. For this purpose we will analyze the scaling properties of the wavelet transform of angle-dependent reflections in seismic data.

Seismic reflection data is best analyzed for its angle-dependent parameters when the data is converted to the Radon-transformed representation $u^{\text{refl}}(p, \tau)$. The Radon transform performs the decomposition into plane waves by stacking along slanted lines in the seismic gather, as recognized and described by Schultz and Claerbout.[4] In this representation the rayparameter is given by $p = \sin \phi(z)/c(z)$. Note that both the local angle of incidence ϕ

and the velocity c are dependent on the depth, whereas the rayparameter p is constant for all depths. This makes it possible to perform analyses of angle-dependency, without knowledge of the velocity function $c(z)$.

The starting point for the analysis is the scalar acoustic wave equation, with $c(z)$ defined by Eq. (2.2):

$$\left[\frac{\partial^2}{\partial z^2} - \left(\frac{1}{c^2(z)} - p^2\right)\frac{\partial^2}{\partial \tau^2}\right] u(z,p,\tau) = 0\,, \tag{3.1}$$

where $u(z,p,\tau)$ is the Radon transform of the pressure field. Replacing z by βz, substituting Eq. (2.3) and multiplying the result by β^2 gives

$$\left[\frac{\partial^2}{\partial z^2} - \left(\frac{1}{c^2(z)} - (\beta^\alpha p)^2\right)\frac{\partial^2}{(\partial \beta^{\alpha-1}\tau)^2}\right] u(\beta z,p,\tau) = 0\,. \tag{3.2}$$

The term between the square brackets is the same as in Eq. (3.1), with p replaced by $\beta^\alpha p$ and τ replaced by $\beta^{\alpha-1}\tau$. Hence, Eq. (3.2) is satisfied by $u(z,\beta^\alpha p,\beta^{\alpha-1}\tau)$ as well as $u(\beta z,p,\tau)$. Consequently,

$$u(z,\beta^\alpha p,\beta^{\alpha-1}\tau) = f(\alpha)u(\beta z,p,\tau)\,, \tag{3.3}$$

where $f(\alpha)$ is an undetermined α-dependent factor. In the upper half-space $z<0$ we define an "incident" wave field u^{inc} and a "reflected" wave field u^{refl}, both obeying Eq. (3.3) with one and the same factor $f(\alpha)$. For our analysis we do not need to specify this "decomposition" any further. We relate these incident and reflected wave fields via a reflection kernel $r(p,\tau)$, according to

$$u^{\mathrm{refl}}(-\epsilon,p,\tau) = \int_{-\infty}^{\infty} r(p,\tau-\tau')u^{\mathrm{inc}}(-\epsilon,p,\tau')\mathrm{d}\tau'\,, \tag{3.4}$$

with $\epsilon \to 0$. When we replace ϵ by $\beta\epsilon$ and substitute Eq. (3.3) for u^{inc} and u^{refl}, we can compare the result with Eq. (3.4), which shows that the reflection kernel $r(p,\tau)$ obeys the following similarity relation

$$r(p,\tau) = \beta^{\alpha-1}r(\beta^\alpha p,\beta^{\alpha-1}\tau)\,. \tag{3.5}$$

We now perform the wavelet transform on $r(p,\tau)$, according to

$$\check{r}(p,\sigma,\tau) = \int_{-\infty}^{\infty} r(p,\tau')\psi\left(\frac{\tau'-\tau}{\sigma}\right)\mathrm{d}\tau'\,. \tag{3.6}$$

Note that in this case we have taken the normalization coefficient $\mu = 0$. Substituting Eq. (3.5), replacing τ' by $\beta^{1-\alpha}\tau'$ and $\mathrm{d}\tau'$ by $\beta^{1-\alpha}\mathrm{d}\tau'$ yields

$$\check{r}(p,\sigma,\tau) = \int_{-\infty}^{\infty} r(\beta^\alpha p,\tau')\psi\left(\frac{\tau'-\beta^{\alpha-1}\tau}{\beta^{\alpha-1}\sigma}\right)\mathrm{d}\tau'\,, \tag{3.7}$$

or, comparing the right-hand side with that of Eq. (3.6),

$$\check{r}(p,\sigma,\tau) = \check{r}(\beta^\alpha p,\beta^{\alpha-1}\sigma,\beta^{\alpha-1}\tau)\,. \tag{3.8}$$

Let $\tau = \tau_{\max}$ denote the τ-value for which $|\check{r}(p,\sigma,\tau)|$ reaches its maximum for fixed p and σ. We define a *modulus maxima plane* as the plane in the (p,σ,τ)-space that connects the local maxima $|\check{r}(p,\sigma,\tau_{\max})|$ for all p and σ. It follows from Eq. (3.8) that the reflection amplitude in a modulus maxima plane behaves as

$$|\check{r}(p,\sigma,\tau_{\max})| = |\check{r}(\beta^{\alpha}p, \beta^{\alpha-1}\sigma, \beta^{\alpha-1}\tau_{\max})|\,. \tag{3.9}$$

The latter equation implies that contours of constant reflection amplitude in a modulus maxima plane are described by

$$p^{1-\alpha}\sigma^{\alpha} = \text{constant}\,. \tag{3.10}$$

Note that for $\alpha = 0$ these contours reduce to straight lines $p =$ constant, hence, any deviation from these straight lines indicates that we are dealing with a singularity, other than the stepfunction.

For the testing of this method, the full acoustic response has been modeled in the velocity function of Fig. 2(a), making use of a reflectivity method. The density has been chosen at a constant value of 2000 kg/m^3 over the complete depth-interval. With some fore-sight the well-log has been chosen such that the first three arrivals are the primaries which are caused by the three self-similar reflectors, with $\alpha = -0.4$, 0 and 0.2 respectively. The left backplane of Fig. 3 shows the prestack depth-migrated dataset $R(p,z)$. It will now be given a third dimension, as visible in Fig. 3, by the continuous wavelet transform according to Eq. (3.6). An artist's impression of the dataset $\check{R}(p,\sigma,z)$ constructed in this way is visible in Fig. 3. The results derived above for the scaling properties of $\check{r}(p,\sigma,\tau)$ apply equally well to this imaged data set.

In Fig. 4 we can see the analytical curves, described by Eq. (3.10) for the three values of α in the (p,σ)-plane, as well as the results obtained from the analysis of the data cube in Fig. 3.

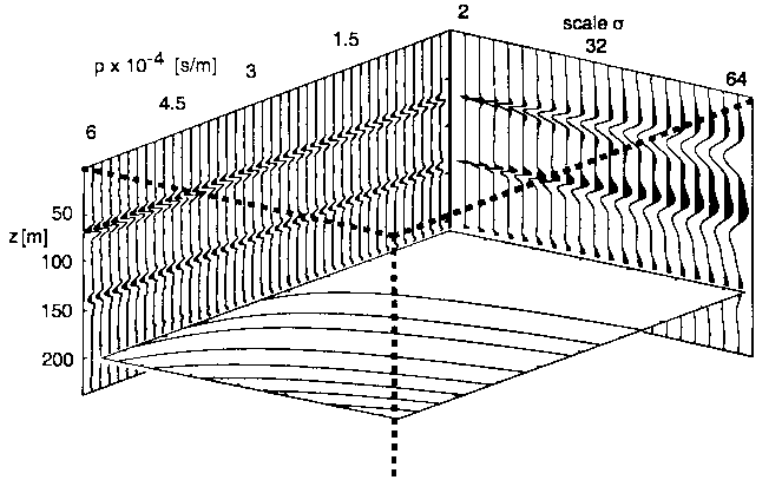

Fig. 3. 3-D representation of the scale analysis on imaged seismic data $\check{R}(p,\sigma,z)$.

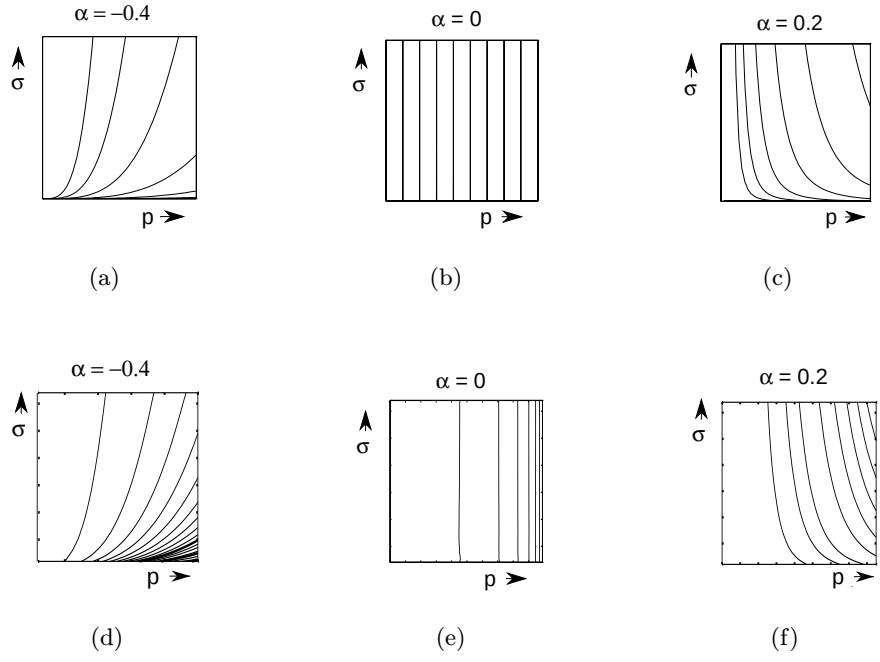

Fig. 4. Analytical contours along which $p^{1-\alpha}\sigma^{\alpha} = \text{constant}$; (a) $\alpha = -0.4$; (b) $\alpha = 0$; (c) $\alpha = 0.2$ and the corresponding results obtained from the image in Fig. 3: (d); (e) and (f).

When we compare the contours obtained from the seismic image with the analytical contours, we can see that the results match very well. This can be quantified by matching the contours of Eq. (3.10) for a range of α-values, which we expect to exist in the data set, with the contours extracted from the seismic data. The matching algorithm consists of the computation of the standard deviation along a set of analytical contours, followed by taking the minimum value of these standard deviations. This will effectively give the best match for α.

The aim of this multi-angle, multi-scale inversion is to resolve the parameters of composite reflectors from the (p, σ)-planes at various depths derived from actual reflection responses. Two examples are shown for seismic data modelled in actual well-logs. Figures 5(a), 5(b) and 5(c) show a multi-scale analysis of a real well-log, analogous to Fig. 2. The slope along the modulus maxima line in Fig. 5(c) ($\alpha = -0.32$) characterizes the singularity at $z = 155$ m in the well-log of Fig. 5(a). Figures 5(d), 5(e) and 5(f) show a multi-angle, multi-scale analysis of the migrated seismic response, analogous to Figs. 3 and 4 (only the angle-dependent reflectivity section and the (p, σ)-plane at $z = 155$ m are shown). Using the contour matching algorithm, it appears that the contours in Fig. 5(f) are approximately described by $p^{1-\alpha}\sigma^{\alpha} = \text{constant}$, with $\alpha = -0.34$. Note that this corresponds very well to the value obtained directly from the well-log. Figure 6 shows a similar example, but this time the analyzed singularity at $z = 170$ m clearly resembles a stepfunction. Note that the contours in Fig. 6(f) show that for this situation there is hardly any scale-dependency, as expected (the contours are approximately described by $p = \text{constant}$).

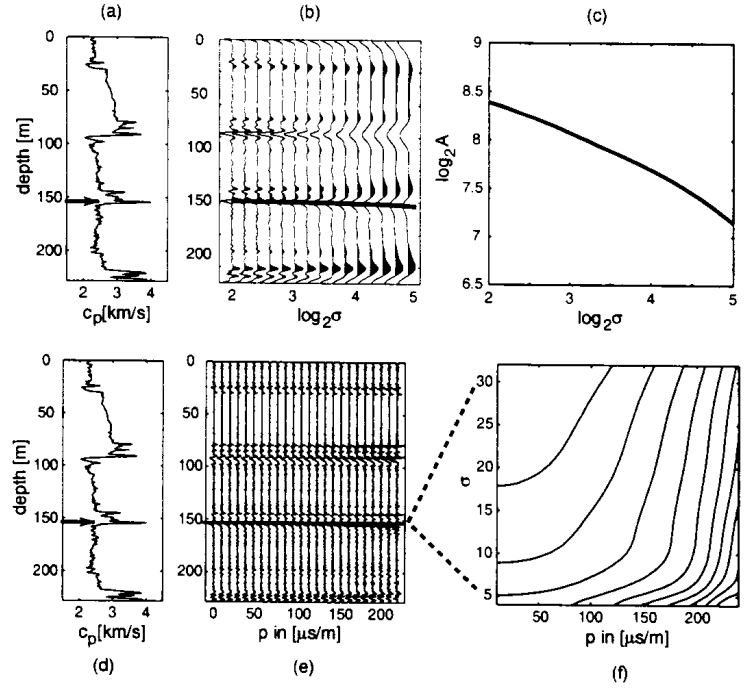

Fig. 5. (a–c) Multi-scale analysis of a singularity in a well-log: $\alpha = -0.32$. (d–f) Multi-angle, multi-scale analysis of its seismic response: $\alpha = -0.34$.

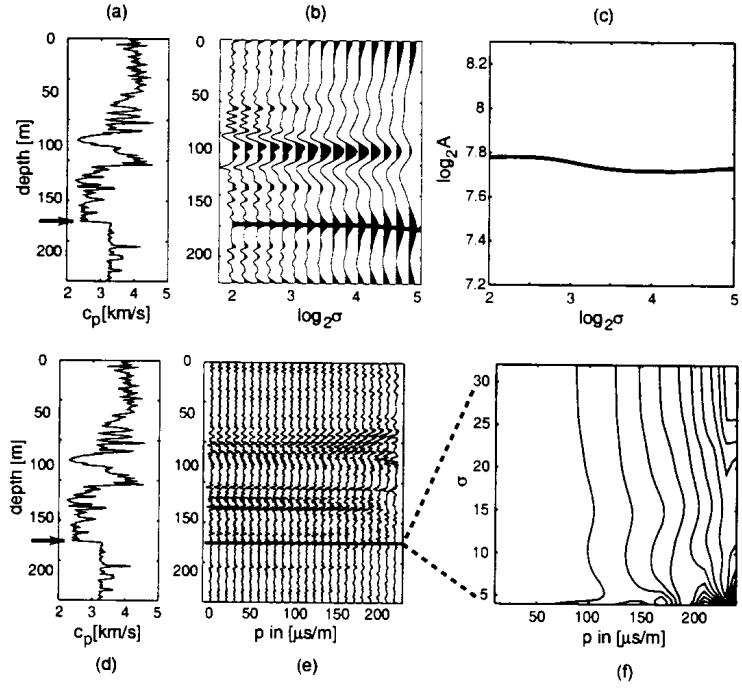

Fig. 6. (a–c) Multi-scale analysis of a stepfunction in a well-log: $\alpha = 0.0$. (d–f) Multi-angle, multi-scale analysis of its seismic response: $\alpha = 0.03$.

4. Conclusions

An alternative parameterization for reflectors in the subsurface has been proposed, which is a generalization of stepfunctions. Reflectors described by this parameterization exhibit a similar multi-scale behavior as several reflectors in real well-logs. It has been shown that the proposed multi-angle multi-scale inversion method provides consistent estimates of the singularity parameter α from synthetic and real well-logs and from seismic data modeled in these well-logs. When looking at the results obtained from the seismic data modeled in the real well-logs, we expect that the singularity exponent α may prove to be a useful seismic indicator. Current research involves the application of this method to real walkaway VSP data by Goudswaard *et al.*[5] and to shallow shear wave seismics by Ghose and Goudswaard.[6]

Acknowledgment

The work reported here was supported by a grant from the Dutch Science Foundation STW (DTN 44.3547). We also thank two anonymous reviewers for their constructive remarks.

References

1. S. G. Mallat and W. L. Hwang, "Singularity detection and processing with wavelets," *IEEE Trans. Inform. Theory* **38**(2), 617 (1992).
2. F. J. Herrmann, *A Scaling Medium Representation*, Ph.D. Thesis, Delft University of Technology, 1997.
3. F. J. Dessing, *A Wavelet Transform Approach to Seismic Processing*, Ph.D. Thesis, Delft University of Technology, 1997.
4. P. S. Schultz and J. F. Claerbout, "Velocity estimation and downward continuation by wavefield synthesis," *Geophysics* **43**, 691 (1978).
5. J. C. M. Goudswaard, M. W. P. Dillen, and C. P. A. Wapenaar, "Multiangle processing and multiscale characterization of walkaway vsp data," in *Soc. Expl. Geophys., Expanded Abstracts* (2000), pp. 178–181.
6. R. Ghose and J. C. M. Goudswaard, "Relating shallow, S-wave seismic to cone penetrating testing (CPT) in soft soil: a multi-angle, multi-scale approach," in *Soc. Expl. Geophys., Expanded Abstracts* (2000), pp. 1331–1334.